DOI: 10.7251/JEPM1902073U
UDC: UDC 539.23:[621.791.92:666.233

Journal of
Engineering & Processing Management

ORIGINAL SCIENTIFIC PAPER

An exploration of the effects of low-pressure plasma discharge on the physicochemical properties of chia (*Salvia hispanica* L.) flour

Rohit Upadhyay[1] | Rohit Thirumdas[2] | Rajendra R. Deshmukh[3] | Uday Annapure[2] | Nrusimha N. Misra[4]

[1]Research & Development, General Mills India Pvt Ltd., Mumbai 79, India

[2]Department of Food Engineering & Technology, Institute of Chemical Technology, Mumbai, India

[3]Department of Physics, Institute of Chemical Technology, Mumbai, India

[4]Department of Engineering, Faculty of Agriculture, Dalhousie University, NS, Canada

Correspondence
N. N. Misra, Tel: +1-(902) 957 9550;
ORCID: 0000- 0001-8041-8893
Email: nn.misra@dal.ca

Abstract

This work explores the preliminary feasibility of employing the low-pressure cold plasma technology for the modification of the properties of chia flour. Chia flour was exposed to low pressure plasma in air for 5 min, 10 min, and 15 min, at two different power levels (40 W and 60 W). The oils extracted from untreated and treated chia flour were exhaustively characterized for fatty acid composition, nutritional value, and rancidity indices using thermal calorimetric methods (DSC/TGA). The results indicated a significant change in the colour of flour with an increase in lightness. Infrared and ultraviolet spectroscopy indicated changes in the tocopherol groups of the oil extracted from plasma treated chia flour. However, the oil extracted from plasma treated chia flour revealed a loss of conjugated dienes and formation of trans-fatty acids as seen in conventional hydrogenation of edible oils. DSC and TGA results revealed better oxidative stability of low-pressure plasma treated oils than control, which was linked to a relative increase of MUFA in the former.

Keywords: electrical discharge, grains, fatty acid, functional property

1. INTRODUCTION

Cold plasma has gained wide attention as an effective surface decontamination and non-thermal food preservation technique. Interestingly, cold plasma (with oxygen in feed gas) is known to induce lipid oxidation in fat containing food products, especially those which are subjected to unsupervised and non-optimized treatment (Gavahian, Chu, Khaneghah, Barba, & Misra 2018). The key mechanism of cold plasma action emerges from the formation of reactive chemical species, *e.g.* reactive oxygen species (ROS), among others, when an electrical field is applied to the working gas, typically air (Misra, Martynenko, et al. 2018). The reactive species hold the key to the preservation properties of NTP; however, in case of ROS, these short-lived species behave as pro-oxidants once permeated into the food products by triggering the chain reaction of lipid oxidation leading to the formation of lipid peroxyl radicals. These peroxyl radicals are primary products of lipid oxidation which get transformed into secondary oxidation compounds which are undesirable from food quality perspective. Hence, while using NTP for high-fat foods, it is critical to ascertain the appropriate dosages which can cause minimal quality alterations. It is equally critical to consider the composition of lipids as high concentration of unsaturated fatty acids (omega −3, 6) renders the food to oxidative rancidity when subjected to plasma treatment (Gavahian et al. 2018).

In the last decade, rising preference for vegetarian/vegan food habits as well as sustainability awareness has led to the global demand for plant-based polyunsaturated oils, which is not catered by most conventional oil seeds. The health foods and nutraceuticals containing bioactive oils (ω-3, 6 rich) from plants sources (*e.g.*, chia and flax seeds) are among most sought-after picks. Chia (*Salvia hispanica* L.), an unconventional oil seed, which is lately touted as a next generation 'wonder' ingredient in the food industry due to its multifunctional health benefits and excellent functional properties as compared to those of other plant-based crops. The uniqueness of chia is that it encapsulates chia oil containing ca. 60% physiologically active ω-3 fatty acids. We selected chia

seeds as the candidate food matrix to understand the effect of plasma treatment (power: 40 and 60 W; treatment time: 5, 10, and 15 min) on its quality using infrared spectroscopy and surface colour (CIE *Lab* system). In addition, we evaluated the stability of mono- and polyunsaturated fatty acids in chia seeds subjected to plasma treatment. The fatty acids composition was analysed via gas chromatography, and oil deterioration was assessed by thermal calorimetric techniques *viz.*, differential scanning calorimetry (DSC) and thermal gravimetric analysis (TGA).

2. MATERIALS AND METHODS

2.1. Experimental set-up

A schematic of the experimental set-up is presented in Figure 1. A bell jar type plasma reactor made of a glass

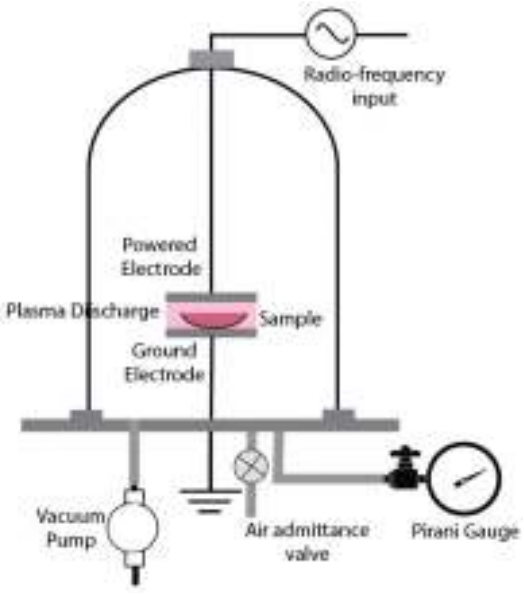

Figure 1. Schematic of the bell-jar type RF plasma experimental set-up

tube having thickness 4 mm, height 120 mm and internal diameter 300 mm was used (Sarangapani et al. 2016; Thirumdas, Trimukhe, Deshmukh, & Annapure 2017). The electrodes were connected through the Wilson seals to the top and bottom stainless-steel plates. The base plate has ports to connect gas/monomer reservoir, pirani gauge, vacuum pump etc. The two parallel electrodes (20 cm diameter) were held 3 cm apart. Atmospheric air (mean temperature of 24±1°C) was used for plasma generation and the working pressure was adjusted to 0.15 mbar using a mass flow controller. Electrodes were capacitively coupled to radio frequency (RF) power supply having a frequency of 13.56 MHz. The matching network was adjusted to obtain a stable glow discharge. The samples were treated at two different power levels of 40 W and 60 W for durations of 5 min, 10 min and 15 min. The output voltage of the power source was measured using a high voltage probe (SEW PD-28 model, attenuation ratio – 1:1000) at the given working pressure. The voltage at 40 W and 60 W was observed to be 1.5 kV and 2 kV respectively. The chia seed powder (10 g) was kept in a petri plate and placed between the two electrodes. Three independent experiments were done for each sample and all the experiments were performed on the same day. The treated samples were designated as control (untreated) sample (vacuum applied without plasma treatment), 40 W – 5 min, 40 W – 10 min, 40 W – 15 min, 60 W – 5 min, 60 W – 10 min, and 60 W – 15 min.

2.2. Fourier Transform Infrared Spectroscopy (FTIR) of chia flour

Chia flour pellet was prepared by diluting 5 mg of chia flour with 195 mg of dry infrared-grade potassium bromide (KBr) and pressing using a manual hydraulic press for 20 min at a pressure of $\sim 10^6$ kg/m^2. The pellet formed was transferred into the FTIR spectrometer (Bruker, Germany) and spectra was recorded in absorbance mode at a resolution of 4 cm^{-1}, over the region 600 to 3500 cm^{-1} by co-adding 32 interferograms. The spectral data was corrected for artefacts and undesirable scatter effect by multiplicative scatter correction (MSC) (Misra, Yong, Phalak, & Jo 2018). The spectral features of the flour were conserved, while background offsets and slopes were largely removed after the MSC. The MSC facilitated the removal of physical effects like particle size and surface blaze from the spectra, which do not carry any chemical or physical information (Misra, Sullivan, & Cullen 2015). The data of each sample was interpreted from the average of three spectra.

2.3. Colour of chia flour

In order to assess the change in colour of plasma treated chia flour, the L* (lightness), a* (redness–greenness) and b* (yellowness–blueness) colour values of control and plasma treated samples were recorded in triplicates using an ultra-scan VIS Hunter Lab colorimeter (Hunter Associates Laboratory Inc., Reston, VA, USA). Prior to measurement of the samples, the instrument was calibrated using white ($L^* = 93.97$, $a^* = 0.88$ and $b = 1.21$) and green ($L^* = 56.23$, $a^* = 21.85$, $b^* = 8.31$) standard tiles.

2.4. UV-VIS spectroscopy of chia seed oil

The transmission spectra of the oil extracted from control and plasma treated chia flour were obtained through ultraviolet-visible spectroscopy. The chia seed oil was

diluted (in 1 : 10 ratio) in spectroscopic grade hexane (De Oliveira et al. 2017). The UV-VIS spectrum was acquired in the 200–600 nm wavelength range using a spectrophotometer (Shimadzu UV 1800, Shimadzu Scientific Instruments) and a quartz cell with a 10 mm path length.

2.5. Fatty acid composition

The fatty acid composition of the oils extracted from plasma treated chia flour was analysed by gas chromatography (TSQ 8000, Thermo Fisher Scientific, Austin, TX, USA) equipped with FID detector. The oils were saponified with 0.5 M NaOH to prepare FAMEs. It was followed by methylation using 40% BF_3 in methanol and later phase partitioning using n-heptane and saturated NaCl solution. A small aliquot (2 μL) of heptane phase was injected (280°C) in GC (split ratio 1 : 30), and fatty acids were resolved by ZB wax column (30 m × 0.25 mm × 0.25 μm). Helium was used as the carrier gas at a flow rate of 1 mL/min. The temperature ramping of the GC oven was done as follows: 60°C for 2 min holding followed by increase to 150°C at 13°C/min for 16 min and finally raised to 240°C at 2°C/min for 10 min. The detector temperature was set at 280°C. FAME standards were used for the calibration and quantification of fatty acids. An index of oxidative stability of oils was determined as calculated oxidisability (COX) using Eq. (1) (Fatemi & Hammond 1980).

$$\mathrm{COX}=\frac{\left[1\times(18:1\%)+10.3\times(18:2\%)+21.6\times(18:3\%)\right]}{100} \quad (1)$$

where, 18 : 1, 18 : 2, and 18 : 3 represented the percentage composition of oleic, linoleic, and α-linolenic acids, respectively.

2.6. Thermogravimetric analysis of chia oil

The thermal stability of extracted chia oils was determined as a function of temperature by thermo-balance (TGA-50, Perkin Elmer Co., Akron, Ohio, USA). The oils (ca. 10 mg) were heated from 35–600°C at 10°C/min under an atmosphere of nitrogen gas (50 mL/min). TG and its derivative plot, known as differential thermal gravimetry (DTG), were used to determine the T_{onset} which marks the initiation of decomposition in oils. The horizontal baseline of TG curve was extrapolated at 1% decomposition, and its intercept with tangent gave T_{onset} (Nik, Ani, & Masjuki 2005). The thermal decomposition of oils was followed in a stepwise regimen to track the associated changes in their mass and degree of unsaturation dependent stability. Considering that the study was intended to understand if low pressure cold plasma treatment results in a change in the physical property of oils, and TG analysis being expensive, the analysis was carried out only for control and samples treated for maximum treatment duration per power.

2.7. Differential Scanning Calorimetry (DSC) of chia oil

Oil induction time (OIT, min) of lipid oxidation exposed to accelerated heating conditions was measured by DSC (DSC Pyris 6, Perkin Elmer Co., Akron, Ohio, USA). Extracted chia oil (ca. 10 mg) was weighed in an open aluminium pan and kept inside the measuring chamber against an empty aluminium pan as a reference. Initially, the oils were studied under dynamic heating regime from 40–600°C and the onset temperature (T_{onset}) of oxidative degradation was noted from DSC curve as an inflection point. Next, the oils were isothermally analysed at $T_{onse} - 10$°C by passing purified oxygen (99.8%) (50 mL/min) and nitrogen (50 mL/min) through sample enclosure. The thermal ramping was programmed as: (1) heat from 40°C to T_{onset} at 10°C/min, (2) hold for 2 min at T_{onset} and then switch the gas to oxygen, and (3) hold for 120 min at T_{onset}. OIT was determined as an intersection of extrapolated baseline and a tangent line of DSC thermograms. Considering that the study was intended to understand if low pressure cold plasma treatment results in a change in the physical property of oils, and DSC analysis being expensive, the analysis was carried out only for control and samples treated for maximum treatment duration per power.

2.8. Statistical analysis

The statistical significance of the difference in mean values of colour parameters with respect to treatment time and plasma power, and their interaction were assessed using a two-way analysis of variance in the **R** statistical software (version 3.4.3).

3. RESULTS AND DISCUSSIONS

3.1. Colour of chia flour

The $L^* - a^* - b^*$ colour parameters of control and plasma treated chia flour are summarized in Table 1. The total colour difference (ΔE) of plasma treated samples with respect to the control are also listed in Table 1. The lightness of the chia flour was found to increase upon plasma treatment, as indicated by an increase in the L^* value. Both applied plasma power and treatment duration were found to be statistically significant ($p < 0.01$) in increasing the lightness (L^*) and decreasing the redness (a^*) of

Table 1. $L^* - a^* - b^*$ colour values of control and plasma treated chia flour. Different superscripted alphabets in the same column indicate statistically significant difference ($p < 0.01$)

Power (W)	Time (min)	L*	a*	b*	ΔE
0	0	30.6 ± 1.6^{a}	4.5 ± 0.2^{a}	12.6 ± 0.1^{a}	–
40	5	38.8 ± 0.6^{b}	4.5 ± 0.1^{a}	15.2 ± 0.2^{b}	8.5 ± 0.8^{a}
40	10	40.3 ± 0.4^{c}	4.3 ± 0.0^{b}	15.0 ± 0.2^{b}	9.9 ± 1.1^{b}
40	15	44.0 ± 0.4^{d}	3.9 ± 0.1^{c}	13.9 ± 0.0^{c}	13.4 ± 1.9^{c}
60	5	40.3 ± 0.8^{c}	4.6 ± 0.1^{d}	15.4 ± 0.1^{b}	10.0 ± 2.3^{d}
60	10	45.9 ± 1.0^{e}	3.7 ± 0.2^{e}	13.4 ± 0.1^{e}	15.3 ± 2.5^{e}
60	15	50.6 ± 0.6^{f}	3.3 ± 0.0^{f}	12.6 ± 0.1^{f}	20.0 ± 0.9^{f}

the flour samples. In an earlier study, an increase in the whiteness of xanthan powder due to oxidizing species was reported after atmospheric pressure plasma treatment (Misra, Yong, et al. 2018). Drawing parallels, the increase in lightness of the plasma treated chia flour was attributed to a bleaching effect and polyphenol breakdown caused by the oxidizing species formed from the electrical discharge in air. The total change in colour (ΔE) was clearly found to be affected by both applied power and treatment duration. For the total colour difference (ΔE), the interaction between applied power and treatment duration was found to be insignificant ($p > 0.05$). However, both the individual independent variables were found to be statistically significant ($p < 0.01$) factors in bringing about the colour change. A higher power results in a larger number of collisions of gas molecules and electrons in air, thereby producing larger quantities of oxidising species. A longer treatment duration, on the other hand, allows greater contact time of the oxidising species with the flour, thus resulting in significant colour changes.

3.2. FTIR spectroscopy

The importance of FTIR spectroscopy in the identification of molecular structures originates from the rich information content obtained and the possibility to assign certain absorption bands related to functional groups. The spectra of the control and plasma treated chia flour are presented in Figure 2. The FTIR spectral features of the control and plasma treated chia flour show considerable overlap due to compositional complexity. Yet, the spectra exhibit several distinct peaks across the entire spectral window. Considerable variability in the intensity of spectral peaks was observed, possibly due to scattering and variable particle sizes that could not be completely eliminated via correction algorithms applied. The broad and most intense peaks at 2854 cm^{-1} and 2927 cm^{-1} originated from symmetric vibrations of (C–H) from phytyl chains and

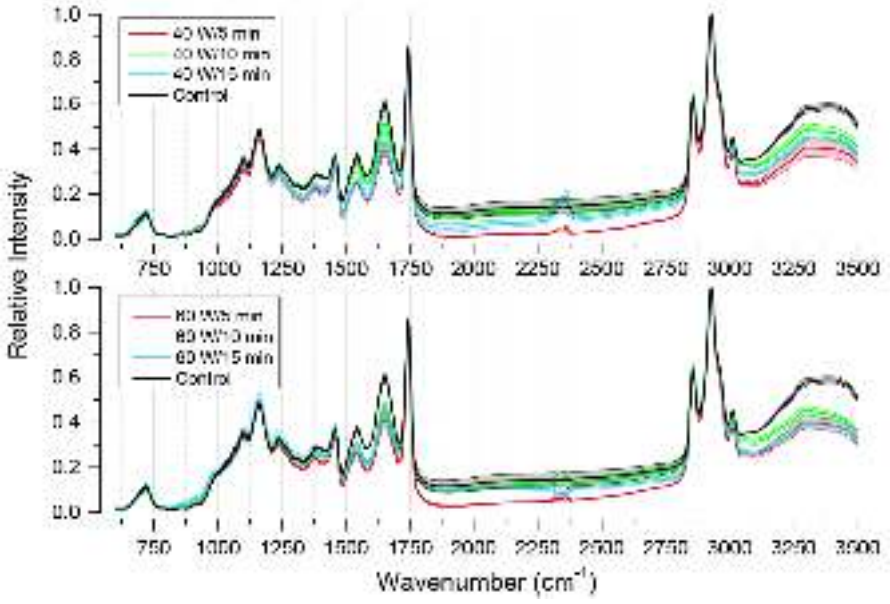

Figure 2. FTIR Spectrum of control and plasma treated chia flour. Top: plasma treatments at 40 W power; Bottom: plasma treatments at 60 W power. The translucent regions around each spectrum represent the standard error of measurement ($n = 3$)

asymmetric vibrations of (C–H) functional groups of tocopherols (Carrión-Prieto et al. 2017). However, the contribution of absorption from water molecules could not be ruled out from the picture. The complementary vibrations of phenolic C–O group in tocopherols was observed at 1546 cm^{-1} and 1240 cm^{-1}. A relative decrease in the peak intensity of the peak associated with phenolic groups of tocopherols was observed in the spectrum of plasma treated flour. This decrease was attributed to the possible interaction of plasma reactive oxygen and nitrogen species (RONS) with the phenolic groups of tocopherols. It is to be noted that the peaks associated with the phytyl chain of tocopherols (about 2900 cm^{-1}) did not show considerable difference in their intensity. The sharp peak noticed at 1744 cm^{-1} was a consequence of vibrations from (CO) ester of terpene alkaloids (Carrión-Prieto et al. 2017). However, minor contribution of vibrations from δ(N–H) (amide III) of proteins to the peak at 1240 cm^{-1} could not be over-ruled. The peak at 1654 cm^{-1} was suspected to have originated from an overlap of vibrations from (C=O) vibrations of quinoid ring and the (N–H), amide I group. The peaks at 1458 cm^{-1} and 1163 cm^{-1} were assigned to $\delta(CH_2)$ and methyl ester (C–O–C) functional groups, respectively (Herrero, Ruiz-Capillas, Pintado, Carmona, & Jimenez-Colmenero 2017). Following plasma treatment, minor changes in the spectrum were noticed around 2300 cm^{-1} wavenumber. However, these changes could not be attributed to any functional group with certainty.

3.3. UV-Vis spectroscopy of chia oil

The UV-Vis transmission spectra of the oils extracted from control and plasma treated chia flour is presented in Fig. 3. The spectra of the plasma treated oil exhibited a decrease in transmission of about 319 nm. The decrease in the transmission was a direct function of the plasma treatment time and the plasma power. This decrease indicated the occurrence of molecular absorption phenomenon in the lipid fraction of flour subjected to plasma treatment. Since the broad 319 nm absorbance peak in UV-VIS spectrum of seed oils originates from phenolic contribution of tocopherols (De Oliveira et al. 2017), the structural transformation of tocopherols in the oil was confirmed. This observation confirms the speculation from FTIR spectroscopy, wherein the possible change in the phenolic structure of tocopherols was suspected.

3.4. Fatty acid composition

The detailed composition of fatty acids in the oils extracted from control and plasma treated chia flour is presented in Table 2. Polyunsaturated fatty acids (PUFA)

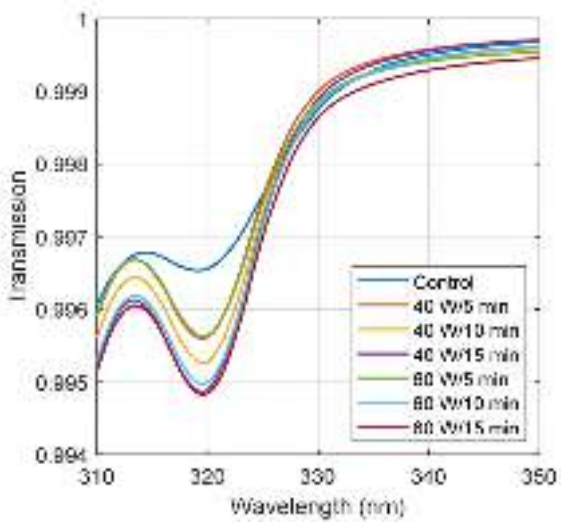

Figure 3. UV-VIS transmission spectra of oil extracted from control and plasma treated chia flour

were seen predominantly with the likes of ω-3 (α-linolenic acid, 60%) and ω-6 fatty acids (linoleic acid, 19.5%) found in control chia oil. The relatively low levels of monounsaturated fatty acids (MUFA, 7%) and saturated fatty acids (SFA, 11%) increases the sensitivity of chia oils to thermo-oxidative rancidity. Polyene index (PI) was used to determine the relative ratio of PUFA and SFA in oils, which can also be an index for nutritional quality of oils, whereas COX index measures the tendency of an oil to get oxidized. The PI and COX values of all the plasma treated oils *vs.* control decreased as a function of plasma treatment dosage and time. The decrease in PI for plasma treated oils is due to their relative decline in PUFA content which eventually reduced their susceptibility to get oxidized, and hence lower COX values were estimated. Notably, the MUFAs are known to withstand the thermal abuse much better than the PUFAs, even before the onset of rancidity (Ghosh, Upadhyay, Mahato, & Mishra 2019). Nonetheless, the decrease in PI values of oils is undesirable from nutritional perspective as it reciprocated to the lowering of PUFA. Furthermore, the better stability of plasma treated oils *vs.* control could also be credited to the relative increase in their MUFA content. Even though an ambitious remark, it might plausibly be due to the plasma induced reduction of conjugated double bonds in fatty acids, which is previously unreported. In addition, our findings revealed the formation of trans-fatty acids (Elaidic acid) in some of the oil samples (A3 and B3) which received high dosage of plasma (40 and 60 W for 15 min, respectively). Although only partially established (Yepez & Keener 2016), these observations shared a certain degree of output features (such as the loss of conjugated dienes and formation of trans-fatty acids) as seen in the conventional hydrogenation of edible oils.

Table 2. Fatty acid composition of oils in raw and plasma-treated chia seeds

Fatty acids	Composition (%)						
	Control (0 W/0 min)	A1 (40 W/5 min)	A2 (40 W/10 min)	A3 (40 W/15 min)	B1 (60 W/5 min)	B2 (60 W/10 min)	B3 (60 W/15 min)
Myristic acid (C14:0)	0.04	0.06	0.06	0.05	0.05	0.06	0.05
Palmitic acid (C16:0)	7.43	8.59	9.26	9.9	8.65	9.92	10.17
Stearic acid (C18:0)	3.94	4.47	5.14	5.88	4.55	5.81	6.37
Oleic acid (C18:1 ω-9 c)	7.06	8.05	8.63	9.80	8.10	9.25	9.96
Elaidic acid (C18:2 ω-9 t)	n.d.	n.d.	n.d.	0.19	n.d.	n.d.	0.24
Linoleic acid (C18:2 ω-6 c)	19.51	21.53	21.79	21.77	21.47	21.80	21.58
α-Linolenic acid (C18:3 ω-3 c)	60.34	55.71	53.28	50.25	55.83	51.00	49.18
ΣSFA	11.41	13.12	14.46	15.83	13.25	15.79	16.59
ΣMUFA	7.06	8.05	8.63	9.80	8.10	9.25	9.96
ΣPUFA	79.85	77.24	75.07	72.02	77.30	72.80	70.76
ΣUFA	86.97	85.29	83.70	82.01	85.40	82.05	80.96
PUFA/MUFA	11.31	9.60	8.70	7.35	9.54	7.87	7.10
Polyene index (PUFA/SFA)	6.99	5.88	5.19	4.55	5.83	4.61	4.27
COX	15.11	14.33	13.84	13.19	14.35	13.35	12.95

n.d. – not detected; ω – nomenclature of fats; c – cis form; t – trans form of fatty acid

While the present work did not prioritize detailed mechanistic investigation to support the anticipated observations, it seems quite reasonable to contemplate this, especially considering the relative increase and decrease in the MUFA and SFA content, and PUFA/MUFA and PI, respectively, of plasma treated oils.

3.5. Thermal stability

The TGA plot of the oils (control, 40 W, 15 min sample, and 60 W, 15 min sample) is illustrated in Fig. 4. A similar thermal trend and plateau were noted between 200 to 350°C for the oils before the onset of decomposition. The T_{onset}, which is interpreted as the onset of mass loss (Δm) or decomposition, had increased in the order 60 W, 15 min sample < 40 W, 15 min sample < control ($p < 0.05$) (Table 2). By virtue of their better thermal stability, the higher SFAs and MUFAs content in plasma treated oils versus control provided them with better thermal stability.

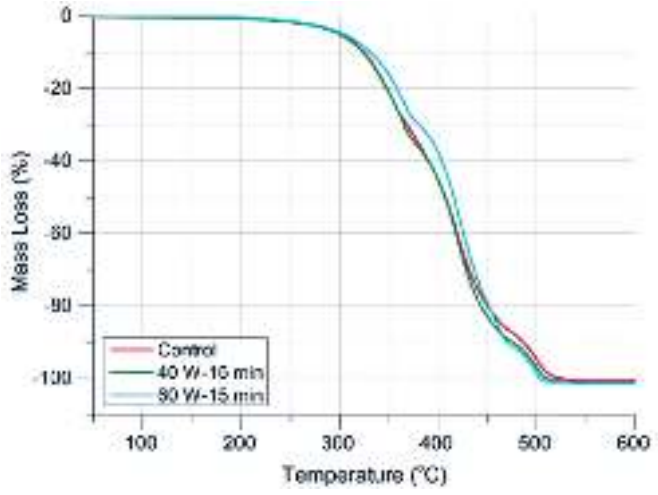

Figure 4. Thermogravimetric plot of the oils

The patterns in DTG plot outlines the different stages in the thermal degradation of oils (Fig. 5). It consisted of 3 tandem steps as follows: step 1 (loss of poly unsaturation, ca. 180–380°C), step 2 (loss of mono unsaturation, ca. 380–480°C), and step 3 (loss of saturation, ca. 480–550°C). The first two steps manifested the decomposition of unsaturated fatty acids (PUFA and MUFA) leading to the generation of short chain fatty acids and volatile carbonyl compounds. This is an important step which

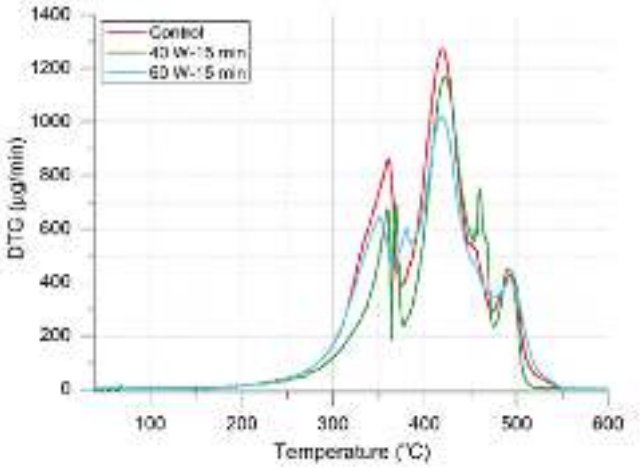

Figure 5. Differential thermogravimetric plot of the oils

Table 3. Thermal decomposition data of oils obtained using TG/DTG and DSC

Oils	Step 1		Step 2		Step 3		T_{onset} (°C)	OIT (min)
	Temperature range (°C)	Δm (%)	Temperature range (°C)	Δm (%)	Temperature range (°C)	Δm (%)		
Control	180–380	32.0	380–455	57.7	455–505	25.6	211.56	12.6
40 W, 15 min	180–368	30.2	368–450	54.2	450–510	22.0	389	15.7
60 W, 15 min	185–370	29.0	370–465	52.3	465–525	19.0	387	16.8

marks the onset of thermally induced rancidity causing alterations in the fatty acid composition of oils. Step-1 and 2 accounted for an overall mass loss (Δm) of 89, 84, and 81% for control, samples treated at 40 W for 15 min, and samples treated at 60 W for 15 min, respectively, which varied per content of their UFAs (87, 82, and 81%, respectively). It was previously noted that control oil had relatively lower MUFAs and SFAs than plasma treated oils, hence it exhibited poor thermal stability and consequently, greater extent of Δm.

The DSC thermograms showed the enthalpy changes due to chemical structural alterations in oils with heating time and temperature (Fig. 6). The thermograms of oils proceeded with an initial endotherm which exhibited an exothermic behaviour upon reaching T_{onset}. In addition, an isothermal DSC facilitated the extrapolation of OIT which followed the order: 60 W/15 min sample (16.8) > 40 W/15 min sample (15.7) > control (12.6) (Table 3). These findings corroborate T_{onset} which revealed the impact of fatty acid composition on thermo-oxidative stability of oils.

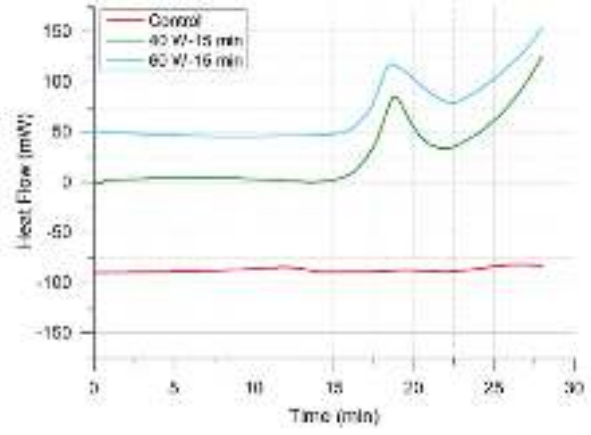

Figure 6. DSC of chia oil samples

4. CONCLUSIONS

Through this work, a preliminary assessment of the effect of low-pressure cold plasma on high omega-3 fat containing chia flour matrix was investigated. Plasma treated chia flour exhibited significant increase in lightness (L*) which was explained by a bleaching effect due to oxidizing species. The FTIR spectroscopy and UV-Vis spectroscopy both confirmed changes in the tocopherols, especially the associated phenolic groups. A voltage-time dependent effect of plasma treatment on the content of omega fatty acids was noted. High plasma power (60 W) applied for longer duration (> 5 min) was more damaging to PUFA ($\omega-3+6$) than MUFA (ω-9). However, the thermal calorimetric analyses (DSC/TGA) revealed that a meticulous voltage-time plasma treatment could be used to induce desired functionality changes in chia seed flour. This in turn might enable creating a thermo-oxidatively improved form of chia oil without being extensively detrimental to ω-3 fatty acids. Furthermore, our findings supported the previous investigations (Yepez & Keener 2016), where plasma assisted hydrogenation of conjugated fatty acids were noted.

REFERENCES

Carrión-Prieto, P., Martín-Ramos, P., Hernández-Navarro, S., Silva-Castro, I., Ramos-Silva, M., & Martín-Gil, J. (2017). Vibrational analysis and thermal behavior of salvia hispanica, nigella sativa and papaver somniferum seeds. *Pharmacognosy Journal*, *9*(2), 157–162. doi: 10.5530/pj.2017.2.26

De Oliveira, I. P., Correa, W. A., Neves, P. V., Silva, P. V., Lescano, C. H., Michels, F. S., … Caires, A. R. (2017). *Optical analysis of the oils obtained from acrocomia aculeata (jacq.) lodd: mapping absorption-emission profiles in an induced oxidation process* (Vol. 4) (No. 4). doi: 10.3390/photonics4010003

Fatemi, S. H., & Hammond, E. G. (1980). Analysis of oleate, linoleate and linolenate hydroperoxides in oxidized ester mixtures. *Lipids*, *15*(5), 379–385. doi: 10.1007/bf02533555

Gavahian, M., Chu, Y.-H., Khaneghah, A. M., Barba, F. J., & Misra, N. (2018). A critical analysis of the cold plasma induced lipid oxidation in foods. *Trends in Food Science & Technology*, *77*, 32–41. doi: 10.1016/j.tifs.2018.04.009

Ghosh, M., Upadhyay, R., Mahato, D. K., & Mishra, H. N. (2019). Kinetics of lipid oxidation in omega fatty acids rich blends of sunflower and sesame oils using rancimat. *Food chemistry*, *272*, 471–477. doi: 10.1016/j.foodchem.2018.08.072

Herrero, A. M., Ruiz-Capillas, C., Pintado, T., Carmona, P., & Jimenez-Colmenero, F. (2017). Infrared spectroscopy used to determine effects of chia and olive oil incorporation strategies on lipid structure of reduced-fat frankfurters. *Food chemistry*, *221*, 1333–1339. doi: 10.1016/j.foodchem.2016.11.022

Misra, N., Martynenko, A., Chemat, F., Paniwnyk, L., Barba, F. J., & Jambrak, A. R. (2018). Thermodynamics, transport phenomena, and electrochemistry of external field-assisted nonthermal food technologies. *Critical reviews in food science and nutrition*, *58*(11), 1832–1863. doi: 10.1080/10408398.2017.1287660

Misra, N., Pankaj, S., Frias, J., Keener, K., & Cullen, P. (2015). The effects of nonthermal plasma on chemical quality of strawberries. *Postharvest biology and technology*, *110*, 197–202. doi: 10.1016/j.postharvbio.2015.08.023

Misra, N., Sullivan, C., & Cullen, P. (2015). Process analytical technology (pat) and multivariate methods for downstream processes. *Current Biochemical Engineering*, *2*(1), 4–16.

Misra, N., Yong, H. I., Phalak, R., & Jo, C. (2018). Atmospheric pressure cold plasma improves viscosifying and emulsion stabilizing properties of xanthan gum. *Food Hydrocolloids*, *82*, 29–33. doi: 10.1016/j.foodhyd.2018.03.031

Nik, W. W., Ani, F., & Masjuki, H. (2005). Thermal stability evaluation of palm oil as energy transport media. *Energy Conversion and Management*, *46*(13-14), 2198–2215. doi: 10.1016/j.enconman.2004.10.008

Sarangapani, C., Thirumdas, R., Devi, Y., Trimukhe, A., Deshmukh, R. R., & Annapure, U. S. (2016). Effect of low-pressure plasma on physico–chemical and functional properties of parboiled rice flour. *LWT-Food Science and Technology*, *69*, 482–489. doi: 10.1016/j.lwt.2016.02.003

Thirumdas, R., Trimukhe, A., Deshmukh, R., & Annapure, U. (2017). Functional and rheological properties of cold plasma treated rice starch. *Carbohydrate polymers*, *157*, 1723–1731. doi: 10.1016/j.carbpol.2016.11.050

Yepez, X. V., & Keener, K. M. (2016). High-voltage atmospheric cold plasma (hvacp) hydrogenation of soybean oil without trans-fatty acids. *Innovative Food Science & Emerging Technologies*, *38*, 169–174. doi: 10.1016/j.ifset.2016.09.001